Photoelectrochemical Characterization of Chalcopyrite $Cu(In_{0.6}Ga_{0.4})_3Se_5$

L. Djellal[a], A. Zahague[a], B. Bellal[b], M. Doulache[b], M. Trari[b*]

[a] *Laboratory of Solid Solutions, Faculty of Physic, (USTHB) BP 32 El Alia 16111 Algiers, Algeria*

[b] *Laboratory of Storage and Valorization of Renewable Energies, Faculty of Chemistry, (USTHB) BP 32 El Alia 16111 Algiers, Algeria*

** e-mail: solarchemistry@gmail.com (M. Trari)*

The compound $Cu(In_{0.6}Ga_{0.4})_3Se_5$ prepared by fusion in sealed tube is a wide band gap semiconductor; it crystallizes in the P-chalcopyrite structure with a direct transition of 1.42 eV. Its transport properties exhibit a semi-conducting behavior, which seem to be not intrinsic but rather attributed to selenium vacancies, and the conductivity is well described by small-polaron hopping: $\sigma = \sigma_0 \exp\{-29/kT\}(\Omega \cdot cm)^{-1}$ with an effective mass of ~ 2 m_0. The thermo-power is negative and changes little with temperature, suggesting that the conduction mechanism is mostly due to electron hopping. The analyzed material shows a chemical stability over a broad pH range; the semi-logarithmic plot in KOH solution displays an exchange current density of 27 $\mu A \cdot cm^{-2}$ and a corrosion potential of -0.204 V_{SCE}. The capacitance measurement (C^{-2}–V) exhibits a linear behavior, characteristic of *n* type conductivity, from which a flat band potential of -0.530 V_{SCE} and an electron density of 3.49×10^{20} cm^{-3} are determined. The Nyquist plot shows a semicircle due to the predominance of the bulk contribution (= 127 $\Omega \cdot cm^2$) and a low density of surface states. The centre is localized below the real axis with a depression angle of 12° ascribed to a constant phase element (CPE). The straight line in the low frequencies region is due to the Warburg diffusion.

Keywords: *chalcopyrite $Cu(In_{0.6}Ga_{0.4})_3Se_5$, small-polaron hopping, photoelectrochemical characterization, electrochemical impedance spectroscopy.*

УДК 544

INTRODUCTION

The past decades have seen a surge of interest into using optically active materials for the solar energy conversion owing to the depletion of fossil energies reserves [1]. We have been attempting to study compounds with a new band structure for the photoelectrochemical (PEC) conversion [2]. Group I-III-VI compounds have attracted considerable attention due to their large scale applications and because they are state-of-the-art power sources for the absorber-layers and solar devices [3]. They have emerged as attractive materials for optoelectronic, photovoltaic devices and PEC cells due to their high absorption coefficients (~ 10^4 cm^{-1}) and moderate surface recombination rates [4]. The progress has been very rapid and today the point is reached when it is necessary to evaluate their physical properties since the reported efficiencies of the incident photon-to-electrical conversion raise the question related to the intrinsic properties.

The growth of defect chalcopyrites in the bulk crystal form has been investigated but, to the best of our knowledge, there are few publications on chalcopyrites containing gallium on the In sublattice [5, 6]. Cells of $CuInSe_2$ have been developed over the past years, achieving the solar cell efficiency close to 19% [7]. The output depends on the band bending at the interface solid/liquid, and *n* type semiconductor should give rise to a large open circuit voltage. In this respect, gallium contributes to the reduction of the electron affinity of the semiconductor and favors the charges separation within the depletion width. A strong difference in the physical properties but close similarity of structures between $CuIn_3Se_5$ and $CuGa_3Se_5$ motivated us to investigate the solid solution and particularly the composition $Cu(In_{0.6}Ga_{0.4})_3Se_5$ because of its band gap of 1.42 eV, close to the ideal value required for terrestrial applications. The present work is devoted to the preparation of $Cu(In_{0.6}Ga_{0.4})_3Se_5$ by direct fusion as well as to the analysis of its physical and PEC properties.

EXPERIMENTAL

Addition of gallium in the ternary system Cu-In-Se is known to easily form additional phases. Through a careful selection of synthesis conditions, it has been found that the composition $Cu(In_{0.4}Ga_{0.6})_3Se_5$ can be prepared in a homogeneous single phase with a slightly modified technique described elsewhere [8]. Ingots are treated in a silica ampoule using programmed speed to preclude selenium loss and oxidation of elements. The silica ampoule containing stoichiometric amounts of Cu, In, Ga and S, all of 5 N purity, is sealed under low

pressure (< 1 mbar), using an inclined growth system. The segregation is precluded by using a thermally controlled furnace, as specified in our previous work on isotypic compounds [2]. The ampoule is heated up to 473 K (300 K·h^{-1}) with an isothermal step of 4 h to permit the reaction of elements with a low melting point. After that, the temperature is raised to 723 K (70 K·h^{-1}), then to 1423 K (11 K·h^{-1}) and is thus maintained for 24 h. The ampoule is first cooled slowly down to 940 K (11 K·h^{-1}) and then quickly (72 K·h^{-1}) to ambient temperature. The phase is identified by X-ray diffraction using Cu K_α radiation in the 2θ range (10–90°) and a step size of 0.1°. The chemical composition is established by the energy dispersive spectroscopy (EDS) at an accelerating voltage of 25 kV. The electrical conductivity is measured on slices cut from the ingot, by the two probe technique, in the temperature range (190–460 K), under argon atmosphere. For the thermo-power, the slice is maintained between two pieces of stainless steel in a sample holder. The thermal gradient (ΔT) is determined by two differential chromel alumel thermocouples, and the electromotrice force (e.m.f.) is measured with a high impedance voltmeter (Tacussel, Aris 2000, 10^{12} Ω). It should be noted that the precision of measurements strongly depends on the quality of the thermal contacts. In our case, an electrical contact is made by soldering copper wires onto the back pellets with silver paint; the linear domain of the ohmic law is automatically checked. The pellets are encapsulated in glass holders leaving an exposed surface area of 0.5 cm^2. The polarization curves and the electrochemical impedance spectroscopy (EIS) are plotted in a standard cell. A platinum electrode (Tacussel, 1 cm^2) and a saturated calomel electrode (SCE) equipped with a lugging capillary serve are auxiliary and reference electrodes, respectively. The potential of the working electrode (WE) is controlled with a PGZ301 potentiostat (Radiometer analytical). Before each run, the working electrode is polished with fine emery paper, degreased with acetone and thoroughly rinsed with water. The support electrolyte (KOH 0.5M) is continually flushed by nitrogen bubbling. The capacitance is measured as a function of the potential at a scan rate of 10 mV·s^{-1}. AC voltage signal of 10 kHz in frequency is applied to the system. The WE is illuminated by a 200 W tungsten lamp equipped with an IR cut off. The light intensity is measured with a digital flux meter (model Testo 545) placed at the same position as the WE. For the EIS, a response analyzer generates 10 mV perturbing signals with the frequencies range of 1 mHz – 100 kHz and subject the WE to various potentials. All solutions are prepared from reagents of the analytical grade quality and demineralized water (~ 1 MΩ·cm).

RESULTS AND DISCUSSION

Compound $Cu(In_{0.6}Ga_{0.4})_3Se_5$ prepared by fusion, crystallizes in the *P* chalcopyrite structure with the space group $I\bar{4}3$ m. The X-ray pattern does not reveal any extra peaks of weak intensity that could have resulted from the ordering between In and Ga atoms (Fig. 1) [9–11]. The refined lattice constants: a = 0.562 nm and c = 1.136 nm, are in good agreement with those in literature [12]. The volume of the unit cell is larger than that of the end member $CuIn_3Se_5$ according to Vegard's law; this simply is attributed to a longer radius of In compared to that of Ga in fourfold coordination. The apparent density (5.54 g·m^{-3}), calculated by the hydrostatic method, is 90% of the theoretical one (5.23 g·cm^{-3}).

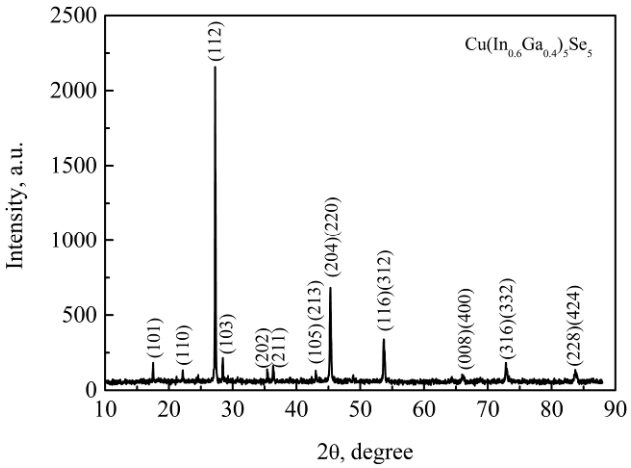

Fig. 1. X-ray diffraction pattern of bulk $Cu(In_{0.6}Ga_{0.4})_3Se_5$.

The morphology, illustrated by SEM micrograph (insert, Fig. 2), clearly shows that $Cu(In_{0.6}Ga_{0.4})_3Se_5$ has a lamellar-type structure. The composition, evaluated with the EDS (Fig. 2), gives the atomic percentages of Cu, In, Ga and Se: 10.39, 20.16, 12.28 and 50.55 at%, respectively, close to the nominal composition. The band gap (E_g) is a dominant parameter of any compound while determining its application for the PEC conversion. The Munk-Kubelka relationship is used to determine E_g from the diffuse reflectance spectrum through [13]:

$$F(R_\infty) = (1 - R_\infty)^2/2\,R_\infty = k/s \qquad (1)$$

$R_\infty = (I/I_0)_{\text{diffuse}}$ is the diffuse reflectivity from an infinitely thick layer (about 2–3 mm), k the absorptivity (cm^{-1}) and s is the scattering factor, independent of the wavelength for particle sizes larger than the wavelength of the incident photon. The gap (= 1.42 eV) is obtained by extrapolating the linear part of $(k/s \cdot h\nu)^{1/2}$ to $h\nu$-axis and the transition is directly allowed (Fig. 3). The observed transition is shifted toward longer energies with respect to $CuIn_3Se_5$. The substitution of Ga for In makes the gap better match the sun spectrum. Such behavior could be explained by the fact that the Ga-Cu bond

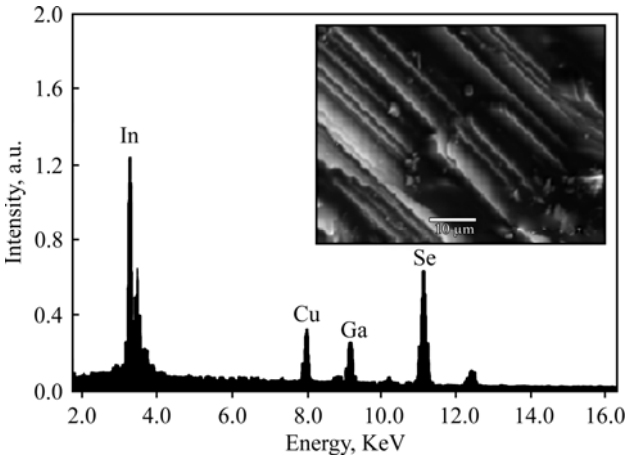

Fig. 2. EDS spectrum of bulk $Cu(In_{0.6}Ga_{0.4})_3Se_5$. Inset: SEM micrograph of $Cu(In_{0.6}Ga_{0.4})_3Se_5$ ingots showing the lamellar structure.

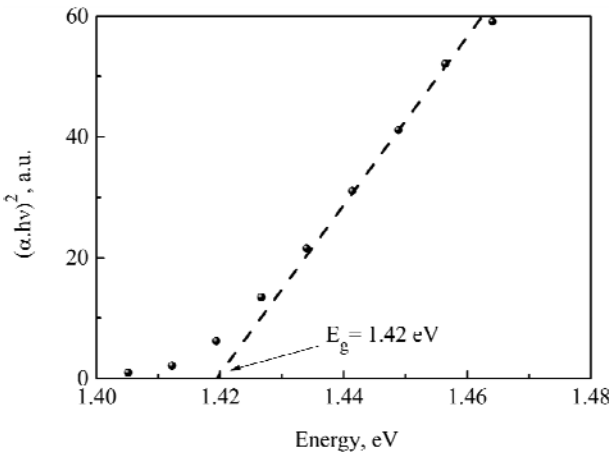

Fig. 3. Direct optical transition obtained by Kubelka-Munk equation.

is more covalent than the In-Cu bond. As gallium is substituted for indium, the width of both the lying valence band and the conduction band increase because of a lower electro-negativity of gallium. If we assume that the conduction band which consists mainly of copper orbital lies approximately at the same energy regardless of the Ga concentration, the broadening of the bands would then be responsible of the larger gap [14]. Each element is tetrahedrally coordinated to four neighboring atoms. The valence band derives from the hybridation of Se: 4*p*/Cu: 3*d* orbitals while the conduction band is made up of Cu: 4*s* states, and the upper valence band is strongly influenced by the *d* metal.

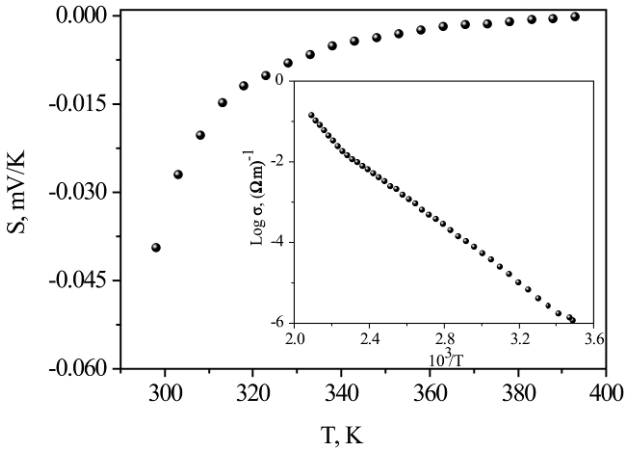

Fig. 4. Thermal variation of thermopower. Inset: Logarithmic plot of conductivity vs. reciprocal temperature.

The transport properties of the compounds under study are dominated by the intrinsic nature and the contribution of the granular structure and minority phases is insignificant due to the robustness of the pellet, a not surprising result since the material is prepared by fusion. The sample is nominally non stoichiometric; the electrical conductivity is monitored by the chemical composition and $Cu(In_{0.6}Ga_{0.4})_3Se_5$ displays semi conducting behavior. The stoichiometric change in the polycrystalline chalcopyrite gives rise to electrically native defects, which in turn provide an increase of the carriers concentration. The exponential dependence of the conductivity on the reciprocal temperature gives activation energy of 29 meV (Fig. 4, insert). Accordingly, nearly all donors are ionized at room temperature (kT ~ 26 meV). Therefore, all electrons are excited over the activation energy and the variation $\sigma(T)$ should result mainly from a thermal activation of the mobility of the carriers localized at the Fermi level (E_F). The electrons supplied by selenium vacancies are mainly responsible of the conductivity and the order of magnitude implies an electrons doping of ~ 10^{19} cm^{-3}.

Such behavior is attributed to the temperature independent density (N_D) in conformity with the thermo power (S) measurement. Indeed, S, defined as the proportionality constant between the temperature gradient and the induced electric potential ($= \Delta V/\Delta T$), is less sensitive to defects states. S is negative, indicating that the majority carriers are electrons and the strong dependence $S(T)$, at least up to ~ 350 K, is at the limit of degenerate conductivity (Fig. 4). In the first hypothesis, an extrinsic generation of electrons would result from a slight selenium deficiency leading, at least formally, to a copper mixed-valence. The Fermi level crosses the mobility edge near the top of the *d*-band, while this composition is probably in the insulating side. The constancy of S above 350 K is attributed to a thermal generation of electrons by impurity ionization (extrinsic process) and, in this case, S is expressed by the equation below [15]:

$$S = k/e\{E_S/kT + B\} = (k/e)\ \mathrm{Ln}\ N_0/N_D. \qquad (2)$$

All constants have their usual meanings; B is a dimensionless constant involving the entropy of transport and can be ignored for small polarons in semiconductors. A large difference between the activation energies E_σ and E_S is a sign of the conduction mechanism by small-polaron hopping, based on the electron lattice interaction. The electron mobility

($\mu_{300\,K} = 1.8 \times 10^{-8}$ V·cm^2·s^{-1}) is calculated from relation ($\sigma = e\ \mu\ N_D$). Hence, an effective mass[1] of ~ $2m_0$ is determined, m_0 being the electron rest mass.

The chemical inertness is an essential requirement for the solar applications. A preliminary test showed that the amount of dissolved copper in the working solution (KOH 0.5M) is too small for a reliable determination by atomic absorption. The stability is due to the fact that the valence band is made up of hybridized Se: 4*p*/Cu: 3*d* orbitals. As noticed above, the deviation from the stoichiometry alters the transport properties and allows us to characterize the material photoelectrochemically. The electrochemistry is a sensitive technique to detect mixed valences in semiconductors. Figure 5 shows the intensity-potential $J(V)$ curve of $Cu(In_{0.6}Ga_{0.4})_3Se_5$ in KOH solution. The material exhibits a good electrochemical stability with a dark current J_d less than 10 μA·cm^{-2}, leading to rectifying the junction at the electrolyte contact (chemical diode). An additional support of the electron localization is brought by the peak corresponding to the electrochemical couple Cu/Cu^{2+} in agreement with our earlier studies [15]. The separation between the anodic (O, 0.62 V) and cathodic (*R*, 0.47 V) peaks is relatively constant and is in the range of ~ 60 mV (~ 0.06/*n*), *n* being the number of exchanged electrons. In addition, the ratio of anodic and cathodic currents is close to unity, indicating a high chemical reversibility. The large current flow below ~ -0.9 V is due to H_2 evolution (gas bubbles were noticeable on the electrode). The chemical stability is supported by the semi logarithmic plot (Fig. 5, insert): in alkaline medium, a corrosion potential of -0.204 V, an exchange current density of 23 μA·cm^{-2} and a polarization resistance 2.18 kΩ·cm^{-2} are determined.

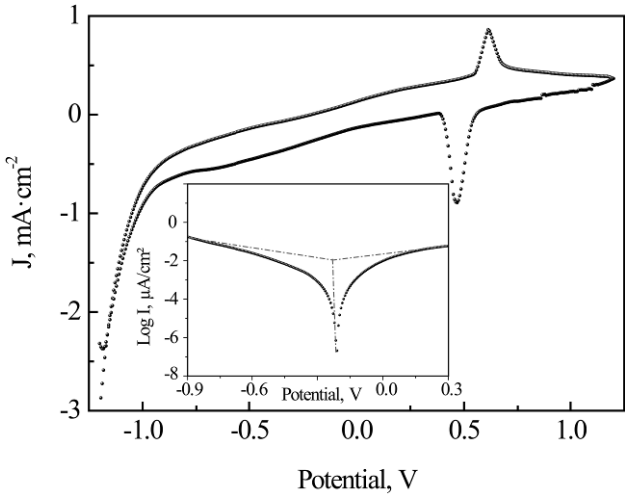

Fig. 5. The cyclic $J(V)$ profile of $Cu(In_{0.6}Ga_{0.4})_3Se_5$ in KOH (0.5M). Inset: semi logarithmic plot of the system.

The photoelectrochemistry gives useful information about the solid state properties of the chalcopyrite. The transient photocurrent-onset-potential (V_{on}), for which J_{ph} appears (-0.50 V) does not vary significantly with pH, confirming the predominant cationic character of the electronic bands; J_{ph} is given by the relation:

$$J_{ph}^2 = \text{const}\alpha^2\delta^2\left(V_{on} - V\right) \qquad (3)$$

δ is the width of the space charge region. The linear plot of J_{ph}^2 intercepts the V-axis at the potential V_{on} (+0.56 V) (Fig. 6, insert). However, the potential V_{fb} is accurately determined from the capacitance measurement:

$$C^{-1} = C_{dl}^{-1} + C_{SC}^{-1} \qquad (4)$$

where C_{dl} is the double layer capacitance and C_{SC} is the space charge capacitance. Due to a low conductivity of $Cu(In_{0.6}Ga_{0.4})_3Se_5$, the approximation $C_{dl} >> C_{SC}$ is valid and the term (C_{dl}^{-1}) can be neglected. Moreover, the selected frequency (10 kHz) is high enough for C_{SC} to dominate the global capacitance, given by the Mott-Schottky equation:

$$C^{-2} = -\left(2 / e\varepsilon\varepsilon_0 N_D\right)\left\{V - V_{fb}\right\} \qquad (5)$$

where all the symbols have their usual significations. The positive slope lends an unambiguous evidence of the *n* type behavior. The potential V_{fb} (-0.530 V) and the electrons density N_D (3.49×10^{20} cm^{-3}) are provided, respectively, from the intercept with the potential axis and the slope of the straight line (Fig. 6). The V_{fb} value should give rise to the large band bending at the interface with a depletion width given by[2]:

$$\delta = \{2\varepsilon\varepsilon_0 (V - V_{fb})/eN_D\}^{0.5}. \qquad (6)$$

The permittivity ε (~ 11) is evaluated from the empirical relation $\varepsilon^2 = 181.8/E_g$ [18]. The potential drop occurs exclusively in the depletion length (δ) which extends over ~ 13 μm^2 because of the low density N_D. The potential difference ($V - V_{fb}$) precludes the loss of (e^-/h^+) pairs and varies to some extent with the semiconductor considered; it represents the band bending at the interface $Cu(In_{0.6}Ga_{0.4})_3Se_5$/electrolyte and an optimal value of 0.5 V is taken, as previously claimed by Gerisher [19]. The EIS is useful for elucidating the electrochemical reactions in heterogeneous charge transfer. The EIS is measured at the open circuit potential (OCP = 0.205 V) by the technique of low perturbation, which allows the system to remain in a state close to the initial one. The Nyquist plot (Fig. 7) exhibits one semi-circle arc attributed to the bulk contribution at the junction $Cu(In_{0.6}Ga_{0.4})_3Se_5$/solution suggesting a single relaxation time of the junction $Cu(In_{0.6}Ga_{0.4})_3Se_5$/electrolyte [20]. The centre lies below the real axis (-12°) and this indicates that the electron hopping occurs by crossing a single potential barrier (intrinsic behavior) which prevails over the grains

[1] $E = (e^4m^*)(16\ \pi\varepsilon\varepsilon_0 h)^{-2}$ where *e* is the electron charge and *h* the Planck constant.
[2] Calculated for an optimal band bending of 0.5 V.

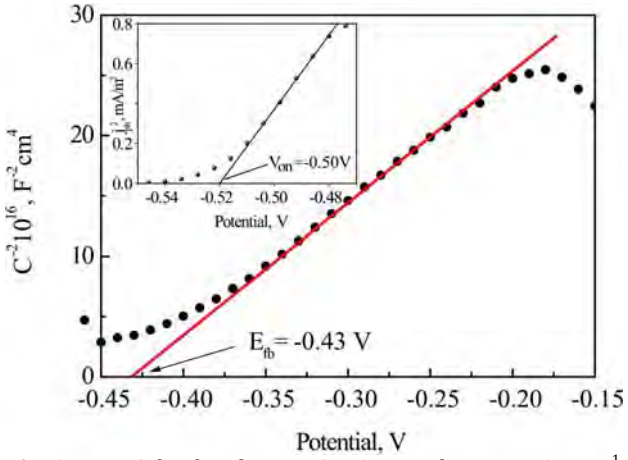

Fig. 6. Mott-Schottky plot in KOH 0.5M solution at 10 mVs^{-1} and 10 KHz. Inset: $J_{ph}^2(V)$ curve.

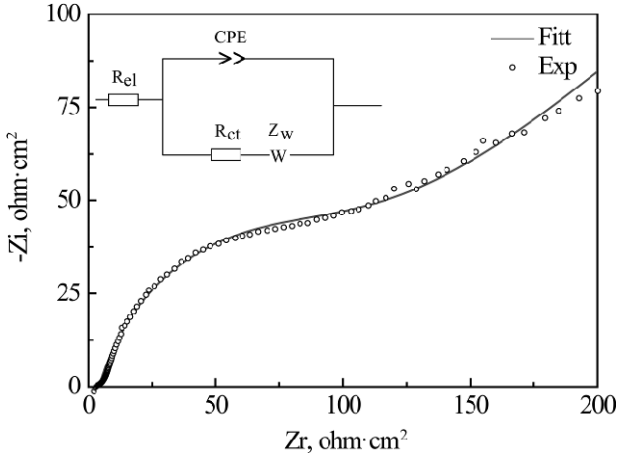

Fig. 7. EIS diagram (Nyquist representation) with fitting plot in KOH (0.5 M) at the free potential. Inset: the equivalent electrical circuit.

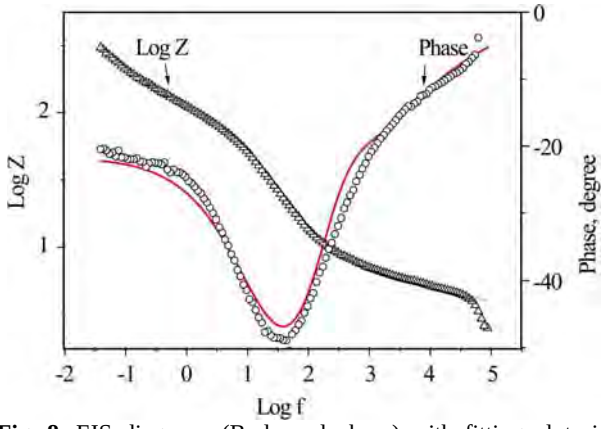

Fig. 8. EIS diagrams (Bode and phase) with fitting plots in KOH (0.5M).

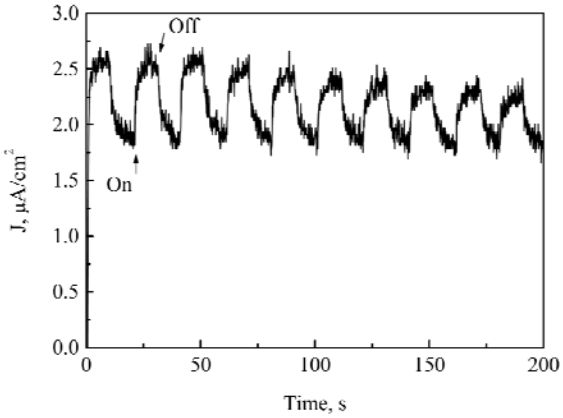

Fig. 9. Time responses of the short circuit current (J_{sc}) under chopped light.

boundaries, a not surprising result owing to the high compactness of the electrode. To take into account the capacitive behavior, a constant phase element (CPE) is introduced by $Q(j\omega)^{-k}$ where k denotes the homogeneity factor ($0 < k \leq 1$) and j the imaginary number ($j^2 = -1$). Figure 8 gives the Bode representation of the same phenomenon. The exchange density is deduced from the relation:

$$J_o = RT/nFR_{ct} \quad (7)$$

(0.1 μA·cm^{-2}) is one order of magnitude lower than that obtained from the semi-logarithmic plot, R_{ct} is the charge transfer resistance (127 Ω·cm^2), F the Faraday constant and T the absolute temperature. The straight line with a slope of 1, in the low frequency range, is due to the Warburg diffusion of the mass transport. The frequency dependence of the impendence of the electrochemical cell is simulated by an equivalent electrical circuit (Fig. 7, insert) composed by a capacitance of the double layer (C_{dl}, 350 μF·cm^{-2}) and the charge transfer resistance (R_{ct}) in series with the Warburg impedance (Z_W) themselves in parallel with CPE, which in turn are connected in series with the resistance of the electrolyte (R_{el}).

A high carriers recombination rate is expected owing to the low electron mobility. So, a high anodic bias is required to induce the transient response. Figure 9 shows the photocurrent time plot under full light illumination. The electrode is biased at the free potential which is more anodic than the potential V_{fb}, the last property is attractive in photocatalysis. The anodic photocurrent confirms the *n* type character of $Cu(In_{0.6}Ga_{0.4})_3Se_5$. However, the photocurrent decays rapidly because the anodic bias is not large enough. This behavior also reflects an electron tunneling from Se: 4*p* valence band to localized holes in copper atoms, which is inhibited at low anodic polarization.

CONCLUSIONS

Chalcopyrite $Cu(In_{0.6}Ga_{0.4})_3Se_5$ has been prepared by fusion from very pure elements. The substitution of gallium for indium is used to increase the gap in order to better match the sun spectrum. Similarly, light absorption begins at higher energies compared to $CuIn_3Se_5$. The deviation from the stoichiometric yields electrically native defects providing improvement of the transport properties. The sign of the thermopower is that of the *n* type carriers whose origin results from selenium vacancies with a low activation energy. The conductivity occurs by small-polaron hopping with an enhanced electron mobility. The photoelectrochemical characterization confir-

med the *n* type behavior. The absence of a right hand semicircle in the electrochemical impedance spectroscopy agrees with the high compactness with a neglected grain boundaries effect. The straight line in the low frequencies domain is due to the Warburg diffusion.

ACKNOWLEDGMENTS

The authors thank Dr G. Rekhila for helpful discussions. This work is supported by the Faculties of Physic and Chemistry of the University of Science and Technology – (USTHB), Algeria.

REFERENCES

1. Saidov M.S. Possibilities of Increasing the Efficiency of Si and $CuInSe_2$. *Solar Cells Applied Solar Energy*. 2011, **47**, 163–165.
2. Djellal L., Bellal B. and Trari M. Physical, Photoelectrochemical Properties of $CuIn_3Se_5$ and Relevance for Hydrogen Production. *Mater Chem Phys*. 2012, **137**, 340–345.
3. Choi I.H. and Lee D.H. Preparation of $CuIn_{1-x}Ga_xSe_2$ Films by Metalorganic Chemical Vapor Deposition using Three Precursors. *Thin Solid Films.* 2007, **515**, 4778–4782.
4. Sebastian P.J., Calixto M.E., Bhattacharya R.N. and Noufi R. CIS and CIGS Based Photovoltaic Structures Developed from Electrodeposited Precursors. *Sol Energy Mater Sol Cells.* 1999, **59**, 125–135.
5. Lehmann S., Fuertes Marryn D., Leyn M., Feyerherm R., Dudzik E., Friedrich E.J., Tovar M., Tomm Y., Wolf C., Schorr S., Schedel-Niedrig Th., Ch. Lux-Steiner M. and Merino J.M. Long-Range Structure of $Cu(In_xGa_{1-x})_3Se_5$: A Complementary Neutron and Anomalous X-ray Diffraction Study. *J Appl Phys*. 2011, **109**, 013518.
6. Levcenko S., Durán L., Gurieva G., Alonso M.I., Arushanov E., Durante Rincón C.A. and León M. Optical Constants of $Cu(In_{1-x}Ga_x)_5Se_8$ Crystals. *J Appl Phys*. 2010, **107**, 033502.
7. Goetzberger A., Hebling Ch. and Schock H.W. Photovoltaic Materials, History, Status and Outlook. *Mater Sci Eng*. 2003, **40**, 1–46.
8. Djellal L., Bouguelia A., Kadi Hanifi M. and Trari M. Physical and Photo Electrochemical Properties of *p*-$CuInSe_2$ Bulk Material. *Sol Energ Mat Sol Cells.* 2008, **92**, 594–600.
9. Wang H.P., Lam W.W. and Shih I. Crystal Growth of $Cu(In_{1-x}Ga_x)_3Se_5$ by Horizontal Bridgman Method. *J Cryst Growth.* 1999, **200**, 137–142.
10. Nomura S. and Endo S. Lattice Dynamics of the Chalcopyrite and Defect Stannite Phases in the Cu–(In, Ga)–Se system. *J Crystal Growth*. 2002, **237**, 2014–2018.
11. Malar P. and Kasiviswanathan S. A Comparative Study of $CuInSe_2$ and $CuIn_3Se_5$ Films using Transmission Electron Microscopy, Optical Absorption and Rutherford Backscattering Spectrometry. *Sol Energ Mat Sol C.* 2005, **88**(3), 281–292.
12. Chang-Dae K., Gye-Choon P., Moon-Seog J. and Duck-Tae K. Structural and Optical Properties of $Cu(In_{1-x}Ga_x)_3Se_5$ Mixed Crystals. *J Korean Physical Society*. 2006, **48**, 951–955.
13. Steven I. Optical Band Gaps of Selected Ternary Sulfide Minerals. *American Mineralogist.* 1998, **83**, 865–871.
14. Marquez R., Rincon C. Defect Physics of the Ordered Defect Compound $CuIn_3Se_5$. *Sol Energ Mat Sol Cells.* 2002, **71**, 19–26.
15. Djellal L., Bouguelia A., Trari M. Structural, Optical and Photo Electrochemical Properties of $CuIn_3Se_5$. *Semicond Sci Techn*. 2008, **23**, 045019–045026.
16. Cattarin S., Guerriero P., Dietz N., Lewerenz H.J. Electrodissolution and Corrosion of $CuInS_2$ Photoanodes with Lamellar Morphology. *Electrochimica Acta*. 1994, **40**(8), 1041–1049.
17. Lide D.R. *Handbook of Chemistry and Physics* 78th Edn. New York: CRC Press, 1997. 2512 p.
18. Roa L., Rincon C., Gonzalez J., Quintero M. Analysis of Direct Exciton Transitions in $CuGa(S_xSe_{1ea})_2$ Alloys. *J Phys Chem Solids.* 1990, **51**(6), 551–555.
19. Gerischer H. Solar Photoelectrolysis with Semiconductor Electrodes. Solar Energy Conversion Topics in Applied Physics. 1979, **31**, 115–172.
20. Manohar Lal, Parshant Kumar Batham, Navdeep Goyal. Complex Impedance and Ac Conductance of $CuInSe_2$. *Sol Energ Mat Sol Cells.* 1995, **36**(2), 111–119.

Received 25.06.13
Accepted 17.12.13

Реферат

Соединение $Cu(In_{0.6}Ga_{0.4})_3Se_5$, полученное синтезом в запаянной трубке, является широкозонным полупроводником, который кристаллизуется, приобретая халькопиритную структуру *p*-типа с прямым переходом 1,42 эВ. При транспорте, проявляются полупроводниковые характеристики полученного соединения, которые не являются его собственными, изначально присущими, а, скорее, приобретенными вследствие наличия вакансий селена; его проводимость хорошо описывается перескоком полярона малого радиуса: $\sigma = \sigma_0 \exp\{-29/kT\}(\Omega \cdot см)^{-1}$, с эффективной массой ~ 2 m_0. Его тепловая энергия отрицательна и почти не изменяется при изменениях температуры, что можно объяснить тем, что механизм теплопроводности зависит от перескоков полярона. Анализируемое соединение обладает химической устойчивостью в широком диапазоне значений pH. Полулогарифмический график в растворе KOH показывает плотность тока при перескоке 27 $\mu A \cdot см^{-2}$ и вероятность коррозии -0,204 V_{SCE}. Емкостное сопротивление (C^{-2}–V) показывает линейное поведение, характерное для проводимости *n*-типа, откуда можно определить вероятность плоской зоны как -0,530 V_{SCE} и плотность электронов как $3{,}49 \times 10^{20}$ $см^{-3}$. На диаграмме Найквиста приведен полукруг из-за преобладания вклада внутренней структуры (= 127 $\Omega \cdot см^2$) и низкой плотности поверхностных состояний. Центр расположен ниже реальной оси, с углом наклона пели 12°, за счет постоянного элемента фазы (ПЭФ). Прямая линия в области низких частот объясняется диффузией Вартбурга.

Ключевые слова: халькопирит $Cu(In_{0.6}Ga_{0.4})_3Se_5$, перескок полярона малого радиуса, фотоэлектрохимические характеристики, электрохимическая импедансная спектроскопия.